

## MIT Open Access Articles

*An Analytic Benchmark for Neutron Boltzmann Transport with Downscattering—Part I: Flux and Eigenvalue Solutions*

The MIT Faculty has made this article openly available. **Please share** how this access benefits you. Your story matters.

**Citation:** Sobes, Vladimir, Ducru, Pablo, Alhajri, Abdulla, Ganapol, Barry and Forget, Benoit. 2021. "An Analytic Benchmark for Neutron Boltzmann Transport with Downscattering—Part I: Flux and Eigenvalue Solutions." Nuclear Science and Engineering, 195 (8).

**As Published:** 10.1080/00295639.2021.1874777

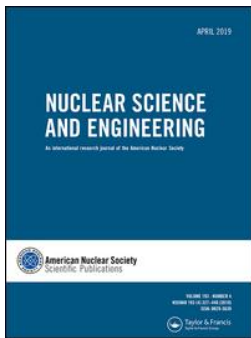
**Publisher:** Informa UK Limited

**Persistent URL:** <https://hdl.handle.net/1721.1/147133>

**Version:** Author's final manuscript: final author's manuscript post peer review, without publisher's formatting or copy editing

**Terms of use:** Creative Commons Attribution-Noncommercial-Share Alike





## An Analytic Benchmark for Neutron Boltzmann Transport with Downscattering—Part I: Flux and Eigenvalue Solutions

Vladimir Sobes, Pablo Ducru, Abdulla Alhajri, Barry Ganapol & Benoit Forget

To cite this article: Vladimir Sobes, Pablo Ducru, Abdulla Alhajri, Barry Ganapol & Benoit Forget (2021): An Analytic Benchmark for Neutron Boltzmann Transport with Downscattering—Part I: Flux and Eigenvalue Solutions, Nuclear Science and Engineering, DOI: [10.1080/00295639.2021.1874777](https://doi.org/10.1080/00295639.2021.1874777)

To link to this article: <https://doi.org/10.1080/00295639.2021.1874777>



View supplementary material [↗](#)



Published online: 23 Mar 2021.



Submit your article to this journal [↗](#)



Article views: 43



View related articles [↗](#)



View Crossmark data [↗](#)



# An Analytic Benchmark for Neutron Boltzmann Transport with Downscattering—Part I: Flux and Eigenvalue Solutions

Vladimir Sobes,<sup>a\*</sup> Pablo Ducru,<sup>b</sup> Abdulla Alhajri,<sup>b</sup> Barry Ganapol,<sup>c</sup> and Benoit Forget<sup>b</sup>

<sup>a</sup>University of Tennessee, 1412 Circle Drive, Knoxville, Tennessee 37996

<sup>b</sup>Massachusetts Institute of Technology, 77 Massachusetts Avenue, Cambridge, Massachusetts 02139

<sup>c</sup>The University of Arizona, 1130 North Mountain Avenue, Tucson, Arizona 85721

Received October 1, 2020

Accepted for Publication January 7, 2021

**Abstract** — Computing in the energy dimension is one of the greatest challenges confronting present-day deterministic neutron transport solvers. Accurately resolving the neutron flux as neutrons downscatter across resonances in the nuclear cross sections currently requires considerable computing power and suffers from approximation errors. Flux uncertainty resulting from the uncertainty of the resonance structure is the single-largest cause of reactivity uncertainty. Any additional reference solution for the critical neutron downscattering problem with resonance phenomena would be a boon to verification and validation of neutronics codes.

This paper establishes a benchmark to verify the accuracy of neutron transport criticality solvers along the energy dimension. For the first time, the analytic solution of the flux amplitude is derived in the particular case of an infinite homogeneous medium with isotropic scattering in the center of mass and an arbitrary number of no-threshold, neutral particle reaction resonances (e.g., radiative capture, fission, and resonance scattering). Original analytic expressions are established to quantify the discrepancy between the  $\psi_k(E)$  and  $\psi_\alpha(E)$  flux amplitudes, respective solutions of the multiplication factor  $k$ , or the exponential time-evolution frequency  $\alpha$  eigenproblems. The physical study of these relations led to analysis of their first-order relative difference near the criticality condition  $\alpha = 0$ . Finally, numerical solutions are provided to a benchmark problem constituted of the first resonance of  $^{239}\text{Pu}$ , the 6.67-eV resonance of  $^{238}\text{U}$ , and a scattering isotope with a flat cross section, allowing for the computational verification of the energy resolution of current neutron transport criticality codes. Through these novel results, this analytic benchmark can serve as a reference to verify the energy resolution and sensitivity analysis of neutron transport criticality calculations.

**Keywords** — Neutron transport, neutron slowing down, nuclear cross-section resonances, resonance self-shielding, analytic benchmark.

**Note** — Some figures may be in color only in the electronic version.

## I. INTRODUCTION: THE NEED FOR A REFERENCE NEUTRON SLOWING-DOWN PROBLEM

Solving the linear Boltzmann transport problem, which dictates the evolution of the angular neutron flux distribution in a nuclear system, is the main challenge of

neutronics.<sup>1–4</sup> The case of a self-sustaining fission chain reaction, called criticality, is particularly important. In this case, the energy dimension is by far the most complex: Neutrons can collide with nuclei and scatter off at a different energy, or they can react with the encountered nucleus to produce new particles. In this process, neutrons slow down from the energy at which they were born, encountering the myriad quantum resonances that make up nuclear cross sections.

---

\*E-mail: [sobesv@utk.edu](mailto:sobesv@utk.edu)

To deal with the energy variable, deterministic neutronics codes perform energy group averaging and spatially solve the Boltzmann transport one energy group at a time. High accuracy is lost through this group-collapsing approximation as it cannot account for the fine resonance structure of nuclear cross sections, which is a phenomenon called resonance self-shielding. Resolving resonance self-shielding is a core challenge of nuclear reactor physics, which has traditionally required resonance models (such as the narrow, wide, or intermediate resonance models as defined in Chap. 8.3 of Ref. 4) and is a field of active research.<sup>5–9</sup> Alternatively, Monte Carlo simulations can follow neutrons continuously through the energy dimension, albeit at a high computational cost.<sup>10–13</sup> This cost is increased further when estimating the flux, which requires an energy grid on which to tally neutron collisions, strongly hindering the statistical resolution of the Monte Carlo simulation when seeking to resolve the resonance self-shielding effect.

The criticality condition of a nuclear system is traditionally expressed either through the rate of exponential time evolution  $\alpha$  or through the multiplication factor  $k$ . For simplicity, most current reactor physics codes solve for the neutron flux  $\psi_k(E)$  of the  $k$  eigenproblem. However, this flux amplitude  $\psi_k(E)$  does not relate to the time evolution of the flux  $\phi(E, t)$  in the system outside of steady state, which is the criticality condition  $k = 1$ . In contrast, the flux amplitude  $\psi_\alpha(E)$  that solves the  $\alpha$  eigenproblem is the dominant mode of time evolution of the system  $\phi(E, t) = \psi_\alpha(E) e^{\alpha t}$  outside the critical regime  $\alpha = 0$ . No analytic benchmark presently quantifies the discrepancy between the  $\psi_k(E)$  and  $\psi_\alpha(E)$  solutions, which is the bias introduced by solving the  $k$  eigenproblem when  $k \neq 1$  and assuming that  $\psi_k(E)$  [instead of  $\psi_\alpha(E)$ ] is the amplitude of the actual flux  $\phi(E, t)$  in the nuclear reactor.

In this analytic benchmark, an infinite homogeneous system is assumed with isotropic scattering and a flat fission spectrum. Integral expressions for the reaction rate are derived, along with the associated  $\alpha$  eigenvalue via an implicit representation, while showing that for the  $k$  eigenvalue, the corresponding relation is explicit. Moreover, these integral expressions can be integrated into closed-form solutions by further assuming that the cross sections are rational functions in momentum space. This holds for 0 K, no-threshold, neutral particle nuclear cross sections. This is the first closed-form resolution of resonance self-shielding phenomena as well as resolution of the discrepancy between the  $\psi_\alpha$  and  $\psi_k$  fluxes.

The objective is to provide a long-lasting contribution by defining an analytically solvable (in continuous energy) critical benchmark problem with resonance cross

sections. The benchmark is defined in Sec. VI. The benchmark cross sections are defined in Table I, with the equations defined in Sec. VI.A. For practical purposes, data files are provided in the ENDF6 format in the online supplement. The benchmark quantities are the  $k$  eigenvalue of unity to less than 1 pcm and the flux. The flux in this benchmark is analytic and is parameterized by poles and residues given in Table III.

Beyond serving as a benchmark problem for a modeling code that is capable of simulating the neutron slowing-down process, the analytic methods developed in this benchmark will be useful in the study of methods and approximations used with multigroup cross-section calculations. One potential use that has not been fully explored is the verification of slowing-down codes used in generating resonance integral tables. Furthermore, the analytic methods proposed here may be explored to find a way to optimize group width selection based on the medium and multigroup approach selected.

## II. NEUTRON SLOWING DOWN: INFINITE HOMOGENEOUS WITH ISOTROPIC SCATTERING

This section begins with the general linear Boltzmann neutron transport equation. The assumptions are established to define the benchmark downscattering problem (Sec. II.A) and to define the corresponding eigenproblems (Sec. II.B). The discussion proceeds to derive and formally solve for the flux and eigenvalues (Sec. II.C) as well as their discrepancies (Sec. II.D) and perturbations (Sec. II.E).

### II.A. Benchmark Problem and Assumptions: Critical Infinite Homogeneous Neutron Slowing-Down Problem

The linear Boltzmann equation, which governs neutron transport in nonrelativistic regimes, is considered:

$$\begin{aligned} & \left[ \frac{1}{v} \frac{\partial}{\partial t} + \Omega \cdot \nabla + \Sigma_t(\mathbf{r}, E, t) \right] \phi(\mathbf{r}, \Omega, E, t) \\ &= \int_0^\infty dE' \int_{4\pi} d\Omega' \Sigma_s(\mathbf{r}, \Omega' \rightarrow \Omega, E' \rightarrow E, t) \phi(\mathbf{r}, \Omega', E', t) \\ &+ \frac{\chi(E)}{4\pi} \int_0^\infty dE' \int_{4\pi} d\Omega' v(E') \Sigma_f(\mathbf{r}, E', t) \phi(\mathbf{r}, \Omega', E', t) \\ &+ Q(\mathbf{r}, \Omega, E, t), \end{aligned} \quad (1)$$

where traditional reactor physics definitions of the variables are used.<sup>2</sup> The main assumptions of the benchmark problem are as follows:

1. time-independent cross sections
2. infinite homogeneous medium (only the energy dimension remains)
3. no external source  $Q(E) = 0$
4. isotropic scattering in the center of mass (COM) from an atomic weight ratio (AWR) of 1, (i.e., implying no Placzek transients (see pp. 213–214 of Ref. 1))
5. The nuclei on which the neutrons scatter cannot transfer their kinetic vibrational energy to the neutrons; that is, there is no upscattering (in practice, this only happens at 0 K temperature).

These assumptions define the benchmark as a purely downscattering problem in energy for which explicit analytic solutions are derived for benchmark purposes.

The assumptions of the infinite homogeneous medium make the problem spatially independent. Removing time dependence in the cross sections and in the external source, the general neutron Boltzmann Eq. (1) now becomes a homogeneous integro-differential equation driven by an initial condition. By convention, the fission spectrum is normalized:  $\int_0^{E_\infty} \chi = 1$ . It is assumed that fission neutrons are born at energies lower than or equal to  $E_\infty$ ; that is,  $\chi(E) = 0$ ,  $E \geq E_\infty$ . Since there is no upscattering and no external source, the flux and the entire equation are cut off at  $E_\infty$ . For this work,  $E_\infty$  is set to 20 MeV, as is conventional in reactor physics.

Furthermore, to allow for direct comparison with Monte Carlo neutron transport solutions, it is assumed that neutrons that downscatter below some lower-energy boundary  $E_0$  are immediately terminated, as is the case with many Monte Carlo neutron transport codes where  $E_0 = 10^{-5}$  eV. In the solution, the lower-energy boundary is completely arbitrary and can be set to zero or any low-energy value where the  $1/v$  behavior of the capture cross section overtakes the fission and elastic scattering cross sections, validating this assumption. Thus, these assumptions establish the following critical infinite homogeneous neutron slowing-down problem:

$$\left[ \frac{1}{v} \frac{\partial}{\partial t} + \Sigma_t(E) \right] \phi(\Omega, E, t) = \int_{E_0}^{E_\infty} dE' \int_{4\pi} d\Omega' \Sigma_s(\Omega' \rightarrow \Omega, E' \rightarrow E) \phi(\Omega', E', t) + \frac{\chi(E)}{4\pi} \int_{E_0}^{E_\infty} dE' \int_{4\pi} d\Omega' v(E') \Sigma_f(E') \phi(\Omega', E', t) \quad [E \in [E_0, E_\infty]] \quad (2)$$

All solutions are valid for  $E \in [E_0, E_\infty]$ . Therefore, explicit notice of this is excluded from the remainder of the paper.

It is assumed that the only scattering that occurs can slow down neutrons to zero energy immediately.<sup>a</sup> In practice, this is never true as the mass of hydrogen is slightly different from the mass of a neutron. All scattering is assumed to be isotropic<sup>b</sup> and from AWR = 1. Therefore,

$$\Sigma_s(\Omega' \rightarrow \Omega, E' \rightarrow E) = \frac{2\mu \Sigma_s(E')}{2\pi E'} \quad (3)$$

where  $\mu$  is the cosine of the polar angle in the COM. Here, we have taken advantage of the fact that a neutron scattering off an  $A = 1$  isotope can lose all of its energy, or in other words, it is equally likely to leave a collision with any energy between 0 and its incoming energy  $E'$ . Since it was assumed that no upscattering can occur (0 K target nuclei), all of these assumptions result in a flux  $\phi$  that is independent of position and direction. Therefore, we are free to integrate over all solid angles. Now, the transport equation is

$$\left[ \frac{1}{v} \frac{\partial}{\partial t} + \Sigma_t(E) \right] \phi(E, t) - \int_E^{E_\infty} dE' \frac{\Sigma_s(E')}{E'} \phi(E', t) = \chi(E) \int_{E_0}^{E_\infty} dE' v \Sigma_f(E') \phi(E', t) \quad (4)$$

where  $v \Sigma_f(E') \triangleq v(E') \Sigma_f(E')$  is written for convenience.

<sup>a</sup> Note that there is no approximation or discrepancy here because neutrons can theoretically downscatter to zero energy whereas the lower-energy boundary in this work has been set to  $E_0 \geq 0$ . Neutrons are allowed to downscatter below energy  $E_0$  if  $E_0 > 0$  is chosen, but here, those neutrons are simply defined to be immediately absorbed.

<sup>b</sup> Isotropic scattering is defined as equiprobable in the cosine of the angle in the COM. This transforms to a probability density function of  $2\mu d\mu$  in the cosine of the scattering angle in the laboratory. Then, the above equation is integrated over  $[0, 2\pi]$  in the azimuthal angle and over  $[0, 1]$  in the cosine of the laboratory angle.

Equation (4) is the final simplification of the time-dependent Boltzmann problem, under the assumptions of zero-dimensional (0-D) (infinite homogeneous medium) energy slowdown from 0 K (temperature of 0 K means no atomic vibrations) hydrogen nuclei ( $A = 1$ ). Given an initial flux condition  $\phi(E, t = 0) = \phi_0(E)$ , the Cauchy-Lipschitz theorem guarantees a unique solution to Eq. (4).

Note that assuming hydrogen-only downscattering—whereby an incoming neutron at energy  $E$  is equally likely to scatter off an  $A = 1$  nucleus to any energy between 0 and  $E$ —is a key assumption of this benchmark (in effect neglecting Placzek transients). Without this assumption, the slowing-down equation would be

$$\begin{aligned} & \left[ \frac{1}{v} \frac{\partial}{\partial t} + \Sigma_t(E) \right] \phi(E, t) \\ & - \frac{1}{1 - \tilde{\alpha}} \int_E^{\min\{E_\infty, E/\tilde{\alpha}\}} dE' \frac{\Sigma_s(E')}{E'} \phi(E', t) \\ & = \chi(E) \int_{E_0}^{E_\infty} dE' v \Sigma_f(E') \phi(E', t) , \end{aligned} \quad (5)$$

where  $\tilde{\alpha} \triangleq \left( \frac{A-1}{A+1} \right)^2$  is the classic lethargy loss [see Eq. (8.50) on p. 422 and the remainder of Chap. 8.3 in Ref. 4]. Though the Cauchy-Lipschitz theorem (generalized to discontinuous distributions) still guarantees Eq. (5) has a unique solution (given an initial flux condition), we were not able to find a clean analytic form for it in the framework of this analytic benchmark.

## II.B. Neutron Downscattering Eigenproblems

It is classical to replace the time-dependent Boltzmann neutron transport problem of Eq. (4) with an eigenproblem to eliminate the time dependence. There are two main ways to do so: the  $\alpha$  eigenproblem and the  $k$  eigenproblem.

### II.B.1. The $\alpha$ Eigenproblem: Exponential Time Evolution

The  $\alpha$  eigenproblem consists of taking the Laplace transform in time of the flux  $\phi(E, t)$  and analyzing each of the Laplace frequencies  $\alpha$  and their corresponding amplitudes  $\psi_\alpha(E)$  or modes:

$$\phi(E, t) = \psi_\alpha(E) e^{\alpha t} . \quad (6)$$

This form explicitly provides the rates of exponential growth or decay of the solutions of the time-dependent Boltzmann Eq. (4).

Plugging the  $\alpha$  Laplace mode in Eq. (6) into the transport equation in Eq. (4) and dividing through by the exponential, we arrive at the  $\alpha$  eigenproblem:

$$\begin{aligned} & \left[ \frac{\alpha}{v} + \Sigma_t(E) \right] \psi_\alpha(E) - \int_E^{E_\infty} dE' \frac{\Sigma_s(E')}{E'} \psi_\alpha(E') \\ & = \chi(E) \int_{E_0}^{E_\infty} dE' v \Sigma_f(E') \psi_\alpha(E') , \end{aligned} \quad (7)$$

from which we proceed to define the  $\alpha$  total cross section:

$$\Sigma_t^\alpha(E) \triangleq \left[ \frac{\alpha}{v} + \Sigma_t(E) \right] . \quad (8)$$

Note that in the semiclassical limit,  $E = \frac{1}{2} m_n v^2$ , with  $m_n$  being the neutron mass. Also, both the  $\alpha$  eigenproblem in Eq. (7) and the  $k$  eigenproblem in Eq. (9) are invariant to multiplication by a constant, so the fluxes can be scaled at will.

The great advantage of the  $\alpha$  eigenproblem (7) is that its solution expresses the dominant mode of the time-dependent Boltzmann Eq. (4), through the Laplace transform Eq. (6), assuming that all fission neutrons are released instantaneously. Indeed, applying the Krein-Rutmann theorem (which generalizes the Perron-Frobenius theorem) to eigenproblem (7) warrants there exists a unique largest real eigenvalue  $\alpha_{dom} \in \mathbb{R}$  and that its associated eigenspace is of dimension one: an eigenline (see Chap. 6 of Ref. 3). Moreover, its corresponding Perron eigenvector  $\psi_{\alpha_{dom}}$  can be chosen to be positive:

$E \in \mathbb{R}$ ,  $\psi_{\alpha_{dom}}(E) \geq 0$ . Furthermore, all the other eigenvectors corresponding to other eigenvalues have positive and negative values. Thus, finding the Perron eigenvalue  $\alpha_{dom}$  yields the dominant and only physical behavior in time of the transient Boltzmann Eq. (4), as the Laplace mode  $\phi(E, t) = \psi_{\alpha_{dom}}(E) e^{\alpha_{dom} t}$  will dominate in time all the other modes of Eq. (6). From this point, the objective is to search for the dominant eigenvalue  $\alpha_{dom}$ , so the superscript will be omitted for better readability, as in  $\alpha_{dom} = \alpha$ .

Since  $\alpha$  is the Laplace frequency of the exponential time evolution of the flux  $\phi(E, t) = \psi(E) e^{\alpha t}$ , an immediate consequence is the following:

1. If  $\alpha < 0$ , the system is subcritical, and the flux exponentially decays over time.
2. If  $\alpha = 0$ , the system is critical, and the flux is time independent.
3. If  $\alpha > 0$ , the system is supercritical, and the flux grows exponentially over time.



### II.B.2. The $k$ Eigenproblem: Global Multiplication Factor

The other standard approach is to replace the time-dependent Boltzmann neutron transport problem shown in Eq. (4) with the multiplication factor  $k$  eigenproblem:

$$\begin{aligned} \Sigma_t(E)\psi_k(E) - \int_E^{E_\infty} dE' \frac{\Sigma_s(E')}{E'} \psi_k(E') \\ = \frac{\chi(E)}{k} \int_{E_0}^{E_\infty} dE' v \Sigma_f(E') \psi_k(E') . \end{aligned} \quad (9)$$

This is a generalized eigenproblem that seeks to answer the following: By what multiplication factor  $k$  should the total number of neutrons generated through fission be divided in order to ensure a steady-state system? By definition, this entails the following classification:

1. If  $k > 1$ , too many neutrons are produced by fission, and the system is supercritical.
2. If  $k = 1$ , the total number of neutrons generated by fission is exactly that to achieve criticality.
3. If  $k < 1$ , there are not enough neutrons to sustain criticality, and the system is subcritical.

The definition in Eq. (8) of the  $\alpha$  total cross section entails that at the very particular point of criticality, where  $\alpha = 0$  and  $k = 1$ , we have  $\psi_k(E) = \psi_\alpha(E)$ . Solving the  $k$  eigenproblem of Eq. (9) is formally identical to solving the  $\alpha$  eigenproblem in Eq. (7): setting  $\alpha = 0$  in Eq. (8) and rescaling the fission source  $F_\alpha$  by  $\frac{1}{k}$ . Henceforth, we proceed to solve the  $\alpha$  eigenproblem given in Eq. (7), establishing in Sec. II.C how to solve both eigenproblems and in Sec. II.D defining how to compare the resulting flux amplitudes  $\psi_\alpha$  and  $\psi_k$ .

### II.C. Solving the $\alpha$ Eigenproblem and the $k$ Eigenproblem

To simplify eigenproblems in Eqs. (7) and (9), the following  $\alpha$  total reaction rate is introduced:

$$R_\alpha(E) \triangleq \Sigma_t^\alpha(E) \psi_\alpha(E) , \quad (10)$$

and its corresponding downscattering rate by means of the downscattering ratio:

$$D_S^\alpha(E) \triangleq \frac{\Sigma_s(E)}{E \Sigma_t^\alpha(E)} , \quad (11)$$

and the rate of neutrons production by means of the fission production ratio:

$$f_v^\alpha(E) \triangleq \frac{v \Sigma_f(E)}{\Sigma_t^\alpha(E)} , \quad (12)$$

so that the Boltzmann transport slowing-down  $\alpha$  eigenproblem in Eq. (7) is simply written as follows:

$$R_\alpha(E) = \int_E^{E_\infty} D_S^\alpha R_\alpha dE + \chi(E) \int_0^{E_\infty} f_v^\alpha R_\alpha dE . \quad (13)$$

To solve the integral  $\alpha$  eigenproblem in Eq. (13), it is assumed that  $\alpha$  and  $R_\alpha$  are solutions and derive an ordinary differential equation that  $R_\alpha$  must necessarily satisfy. The total neutron production by fission is denoted

$$F_\alpha \triangleq \int_0^{E_\infty} f_v^\alpha R_\alpha dE , \quad (14)$$

and the Boltzmann transport  $\alpha$  eigenproblem in Eq. (13) is differentiated to yield the integro-differential form:

$$\frac{dR_\alpha}{dE}(E) = -D_S^\alpha R_\alpha(E) + F_\alpha \frac{d\chi}{dE}(E) .$$

It is assumed that there is a cutoff energy  $E_\infty$  past which the spectrum is zero:  $\chi(E > E_\infty) = 0$ , and so is the reaction rate:  $R_\alpha(E > E_\infty) = 0$ . Therefore, the latter integro-differential equation can be generically solved through an integrating factor as follows:

$$R_\alpha(E) = F_\alpha \int_{E_\infty}^E \frac{d\chi}{dE}(E') e^{\int_E^{E'} D_S^\alpha dE''} dE' , \quad (15)$$

on which a further integration per parts, recalling that  $\chi(E \geq E_\infty) = 0$ , yields the following:

$$R_\alpha(E) = F_\alpha \left[ \chi(E) + \int_E^{E_\infty} \chi(E') D_S^\alpha(E') e^{\int_E^{E'} D_S^\alpha dE''} dE' \right] . \quad (16)$$

For brevity of future forms, the differential  $dE''$  will be omitted in the integral of the  $D_S^\alpha$  factor in the exponent.

Solutions in Eq. (15) or Eq. (16) are necessary forms to satisfy the slowing-down problem in Eq. (13). To be sufficient, they must solve the eigenproblem. This can be verified in an integral fashion by multiplying the left and right sides of Eq. (13) by  $f_v^\alpha$  and integrating over  $\mathbb{R}_+$ ,

$$1 = \int_0^{E_\infty} f_v^\alpha(E) \int_{E_\infty^+}^E \frac{d\chi}{dE}(E') e^{\int_E^{E'} D_S^\alpha} dE' dE, \quad (17)$$

or, equivalently (by integration by parts),

$$1 = \int_0^{E_\infty} f_v^\alpha(E) \left[ \chi(E) + \int_E^{E_\infty} \chi(E') D_S^\alpha(E') e^{\int_E^{E'} D_S^\alpha} dE' \right] dE. \quad (18)$$

This is an implicit equation on the  $\alpha$  eigenvalue.

For the  $k$ -eigenvalue problem, the same approach shows that the equation is explicit:

$$k = \int_0^{E_\infty} f_v(E) \int_{E_\infty^+}^E \frac{d\chi}{dE}(E') e^{\int_E^{E'} D_S} dE' dE, \quad (19)$$

$$k = \int_0^{E_\infty} f_v(E) \left[ \chi(E) + \int_E^{E_\infty} \chi(E') D_S(E') e^{\int_E^{E'} D_S} dE' \right] dE, \quad (20)$$

and the  $k$  total reaction rate is simply obtained by setting  $\alpha = 0$  and introducing the eigenvalue  $k$ :

$$\begin{aligned} R_k(E) &= \frac{F_k}{k} \int_{E_\infty^+}^E \frac{d\chi}{dE}(E') e^{\int_E^{E'} D_S} dE' \\ &= \frac{F_k}{k} \left[ \chi(E) + \int_E^{E_\infty} \chi(E') D_S(E') e^{\int_E^{E'} D_S} dE' \right]. \end{aligned} \quad (21)$$

## II.D. Discrepancy Between the $R_\alpha(E)$ and $R_k(E)$ Total Reaction Rates

Of course, when  $\alpha = 0$  (which is equivalent to  $k = 1$ ), the  $\alpha$  reaction rates are the same as the  $k$  reaction rates. In the framework of this analytic benchmark, this discrepancy can be analytically quantified  $R_\alpha(E) \neq R_k(E)$  when  $k \neq 1$ .

From the general forms in Eqs. (15) and (21), if the reaction rates are made commensurate by fixing the same total number of neutrons produced from fission,

$$F_\alpha = \frac{F_k}{k} =: F, \quad (22)$$

then the same physical system—cross sections  $\Sigma$ —will entail that the difference between the  $R_\alpha(E)$  and  $R_k(E)$  reaction rates is as follows:

$$R_\alpha(E) - R_k(E) = F \int_{E_\infty^+}^E \frac{d\chi}{dE}(E') \left[ e^{\int_E^{E'} D_S^\alpha} - e^{\int_E^{E'} D_S} \right] dE'.$$

Given the fixed set of cross sections  $\Sigma$ , the Taylor expansion of the downscattering ratio in Eq. (11) near criticality yields

$$D_{S\Sigma}^\alpha(E) \underset{|\alpha| \ll 1}{\simeq} D_{S\Sigma}^{\alpha=0}(E) + \alpha \frac{\partial D_{S\Sigma}^{\alpha=0}}{\partial \alpha}(E) + \mathcal{O}(\alpha^2), \quad (23)$$

which entails, near critically, that the first-order discrepancy between the  $\alpha$  and  $k$  reaction rate is proportional to  $\alpha$ , and its energy dependence is given by

$$\begin{aligned} \frac{1}{F} [R_{\alpha,\Sigma} - R_{k,\Sigma}](E) &\underset{|\alpha| \ll 1}{\simeq} \\ &\alpha \int_{E_\infty^+}^E \frac{d\chi}{dE}(E') e^{\int_E^{E'} D_S} \left[ \int_E^{E'} \frac{\partial D_S^{\alpha=0}}{\partial \alpha} dE' \right] dE'. \end{aligned} \quad (24)$$

The relationship in Eq. (24) describes the difference between solving the  $k$  eigenproblem in Eq. (9) instead of the  $\alpha$  eigenproblem in Eq. (13) near criticality for a given set of cross sections  $\Sigma$ .

## II.E. Perturbations to the $R_\alpha(E)$ and $R_k(E)$ Total Reaction Rates

The effect that a perturbation to the physical system,  $\Sigma \rightarrow \Sigma + \delta\Sigma$ , has on the  $R_\alpha(E)$  and  $R_k(E)$  total reaction rates can also be studied. The infinitesimal perturbation of the cross sections  $\delta\Sigma$  will induce an infinitesimal perturbation of the  $\alpha$  eigenvalue,  $\alpha \rightarrow \alpha + \delta\alpha$ , through the implicit Eq. (17). Considering the corresponding eigenvector  $R_\alpha$  in Eq. (15), it depends on both the total neutron production by fission  $F_\alpha$ —which includes the fission production ratio of Eq. (12) through Eq. (14)—and the downscattering ratio of Eq. (11). However, in the generalized eigenproblem in Eq. (7), the reaction rate  $R_\alpha$  is defined up to an arbitrary multiplicative constant. To make  $R_\alpha$  and  $R_k$  commensurate, a multiplicative constant is set for both through Eq. (22). Here,  $R_\alpha$  and  $R_{\alpha+\delta\alpha}$  must be made commensurate. To accomplish this, a normalization condition must be prescribed on the reaction rates to study the effect of a perturbation. Here,



the total number of neutrons produced by fission in Eq. (14) is fixed so that under a perturbation, we have

$$\delta F \triangleq \delta F_\alpha = \delta \left( \frac{F_k}{k} \right) \equiv 0 . \quad (25)$$

Note that imposing this normalization condition is possible because  $F$  from Eq. (22) is not a fixed quantity. It is defined in Eq. (14), where the reaction rate  $R_\alpha$  is defined to any arbitrary multiplicative constant.  $R_\alpha$  will still solve the Eq. (7) eigenproblem.

Under this choice of normalization in Eq. (25), the only remaining quantity in Eq. (15) to change under perturbation is the downscattering ratio  $\delta D_{S\Sigma}^{\alpha, \Sigma+\delta\Sigma}(E)$ , where the partial Taylor expansion of Eq. (23) must be modified to account for the total differential:

$$\begin{aligned} D_{S\Sigma+\delta\Sigma}^{\alpha+\delta\alpha}(E) &\simeq D_{S\Sigma}^\alpha(E) + \delta D_S(E) + \mathcal{O}(|\delta D_S(E)|) \\ &= D_{S\Sigma}^\alpha(E) + \delta\alpha \frac{\partial D_{S\Sigma}^\alpha}{\partial \alpha}(E) + \delta\Sigma \frac{\partial D_{S\Sigma}^\alpha}{\partial \Sigma}(E) \\ &\quad + \mathcal{O}(\alpha^2 + \delta\Sigma^2), \\ &\text{for } |\delta\alpha| \ll 1, |\delta D_S(E)| \ll 1 . \end{aligned}$$

Differentiating the  $\alpha$  total reaction rate  $R_\alpha$  in Eq. (15) thus yields the following:

$$\delta R_{\alpha, \Sigma}(E) = F_\alpha \int_{E_\infty}^E \frac{d\chi}{dE}(E') e^{E' D_{S\Sigma}^\alpha} \left[ \int_E^{E'} \delta D_{S\Sigma}^\alpha dE' \right] dE' .$$

If the change in cross section  $\delta\Sigma$  is assumed to be due to a change in a scalar parameter (i.e., not a function of energy), then this entails that the change in reaction rates from a perturbation can be expressed as follows:

$$\begin{aligned} \frac{\delta R_{\alpha, \Sigma}}{\delta \Sigma}(E) &= F_\alpha \int_{E_\infty}^E \frac{d\chi}{dE}(E') e^{E' D_{S\Sigma}^\alpha} \\ &\quad \left[ \int_E^{E'} \frac{\partial D_{S\Sigma}^\alpha}{\partial \Sigma} + \left( \frac{\delta\alpha}{\delta\Sigma} \right) \frac{\partial D_{S\Sigma}^\alpha}{\partial \alpha} \right] dE' , \end{aligned} \quad (26)$$

where  $(\frac{\delta\alpha}{\delta\Sigma})$  is the differential of the  $\alpha$  eigenvalue. Unfortunately, this differential cannot be obtained by simply taking the total differential of the implicit Eq. (17) since the value of  $F_\alpha$  is arbitrary and undefined by Eq. (14) and Eq. (25). To compute the differential  $(\frac{\delta\alpha}{\delta\Sigma})$ , one must differentiate the Boltzmann Eq. (13) and use the adjoint flux theory to solve the resulting Fredholm problem.

Remarkably, when the perturbation is performed on the  $k$  eigenproblem, the downscattering ratio does not depend on  $k$ . Therefore, unlike in Eq. (26), the differential  $(\frac{\delta k}{\delta\Sigma})$  does not appear in the perturbed reaction rate, which is still under normalization condition as shown in Eq. (25):

$$\frac{\delta R_{k, \Sigma}}{\delta \Sigma}(E) = \frac{F_k}{k} \int_{E_\infty}^E \frac{d\chi}{dE}(E') e^{E' D_{S\Sigma}^\alpha} \left[ \int_E^{E'} \frac{dD_{S\Sigma}^\alpha}{d\Sigma} \right] dE' . \quad (27)$$

### III. PARTICULAR CASE OF STEP FISSION SPECTRUM $\chi(E)$

To further solve the integral expressions previously derived, the additional assumption of a step-function (Heaviside, denoted by 1) fission spectrum is introduced:

$$\chi(E) \triangleq \chi_0 1[E < E_\infty] . \quad (28)$$

To be normalized,  $\chi_0 \triangleq \frac{1}{E_\infty}$  is needed so that taking its derivative yields  $\frac{d\chi}{dE}(E') = -\chi_0 \delta(E' - E_\infty)$ , where  $\delta$  denotes the delta distribution. Under this step fission spectrum assumption, the general integral equations established in Sec. II yield much simpler forms:

1. Equation (15) simplifies to

$$R_\alpha(E) = \chi_0 F_\alpha e^{E D_{S\Sigma}^\alpha} . \quad (29)$$

2. Equation (17) simplifies to

$$1 = \chi_0 \int_0^{E_\infty} f_v^\alpha(E) e^{E D_{S\Sigma}^\alpha} dE . \quad (30)$$

3. Equation (20) simplifies to

$$k = \chi_0 \int_0^{E_\infty} f_v(E) e^{E D_S} dE . \quad (31)$$

4. The discrepancy Eq. (24) simplifies to

$$\frac{1}{F} [R_{\alpha, \Sigma} - R_{k, \Sigma}](E) \underset{|\alpha| \ll 1}{\simeq} \alpha \chi_0 e^{E D_S} \left[ \int_E^{E_\infty} \frac{\partial D_{S\Sigma}^{\alpha=0}}{\partial \alpha} \right]$$

so that using Eq. (29), we have

$$\frac{R_{\alpha,\Sigma} - R_{k,\Sigma}}{R_{k,\Sigma}}(E) \underset{|\alpha| \ll 1}{\simeq} \alpha \int_E^{E_\infty} \frac{\partial D_S^{\alpha=0}}{\partial \alpha} . \quad (32)$$

Using Eq. (29), perturbation Eq. (26) simplifies to the following:

$$\frac{1}{R_{\alpha,\Sigma}} \frac{\partial R_{\alpha,\Sigma}}{\partial \Sigma}(E) = \int_E^{E_\infty} \left[ \frac{\partial D_{S\Sigma}^\alpha}{\partial \Sigma} + \left( \frac{\delta \alpha}{\delta \Sigma} \right) \frac{\partial D_{S\Sigma}^\alpha}{\partial \alpha} \right] . \quad (33)$$

If the near-criticality condition  $|\alpha| \ll 1$  is further assumed, then further Taylor expansions can be performed to estimate the latter around  $\alpha = 0$ , and the same results readily apply to the  $k$  reaction rate in Eq. (27), yielding

$$\frac{1}{R_{k,\Sigma}} \frac{\partial R_{k,\Sigma}}{\partial \Sigma}(E) = \int_E^{E_\infty} \frac{dD_{S\Sigma}}{d\Sigma} . \quad (34)$$

Note that it is possible to generalize all these results to box spectra: a piecewise flat (in outgoing neutron energy) fission spectrum  $\chi(E) \triangleq \frac{1}{E_\infty - E_0}$ , for  $[E_0, E_\infty] \in \mathbb{R}_+$ , where  $E_0$  and  $E_\infty$  are the minimum and maximum energies, respectively. One could thus assume a specific compact-supported stepwise spectrum,

$$\chi(E) = \sum_{i=-1}^{N_\infty} \chi_i 1[E \in [E_i, E_{i+1}]] , \quad (35)$$

where  $E_{-1} \triangleq 0$ ,  $\chi_{-1} \triangleq 0$ , and  $E_{N_\infty+1} \triangleq \infty$ ,  $\chi_{N_\infty} \triangleq 0$  are denoted for convenience. Therefore, this stepwise function allows a smooth spectrum  $\chi(E)$  to be approximated to within any target accuracy.

#### IV. PARTICULAR CASE OF RATIONAL 0 K CROSS SECTIONS $\sigma(E)$

All the simplified equations from Sec. III involve the primitive integrals of the downscattering ratio  $D_S^\alpha(E)$  or its partial derivatives. Closed-form solutions to these equations can be derived by introducing a final assumption whereby cross sections  $\sigma(E)$  are rational fractions in  $\sqrt{E}$ . It can be shown from nuclear physics—in particular, R-matrix theory of nuclear interactions<sup>14,15</sup>—that this is always verified at temperature 0 K for neutral particles without threshold in the case of semiclassical R-matrix

theory. Moreover, locally expanding nuclear cross sections in rational fractions is the object of the recently developed Windowed Multipole Library.<sup>16,17</sup>

The generic slowing-down reaction rates and eigenvalue solutions in Eqs. (15) and (17) show that the energy dependence is principally captured by the exponential of the downscattering ratio integral:

$$\mathcal{I}_E^{E'} \triangleq \int_E^{E'} D_S^\alpha(E'') dE'' = \int_E^{E'} \frac{\Sigma_s(E'')}{E'' \Sigma_t^\alpha(E'')} dE'' , \quad (36)$$

while the discrepancy relations, as well as the perturbation relations, depend on the integral of the partial differentials of the downscattering ratio:

$$\mathcal{J}_{\alpha E}^{E'} \triangleq \int_E^{E'} \frac{\partial D_S^\alpha}{\partial \alpha}(E'') dE''$$

and

$$\mathcal{J}_{\Sigma E}^{E'} \triangleq \int_E^{E'} \frac{\partial D_S^\alpha}{\partial \Sigma}(E'') dE'' . \quad (37)$$

#### IV.A. Pole Representation of Neutral Particle 0 K Cross Sections and Downscattering Ratios

In the case of no-threshold neutron reaction cross sections, the angle-integrated cross section can be expressed as the sum of the absorption cross section, which counts all reaction channels and the scattering cross section,  $\Sigma_t(E) = \Sigma_s(E) + \Sigma_a(E)$ . The reaction channels are rational fractions in  $\sqrt{E}$  with simple poles and residues and an asymptotic behavior  $\Sigma_a(E) \underset{E \rightarrow 0}{\sim} 1/\sqrt{E}$ , so it has a pole expansion as follows:

$$\Sigma_a(E) = \frac{1}{\sqrt{E}} \Re \left[ \sum_{j=1}^J \frac{r_j^{c,a}}{\sqrt{E} - p_{a,j}} \right] , \quad (38)$$

where  $J$  is finite and can be determined based on the number of energy levels of the cross section, and the orbital angular momentum of the incoming channel.<sup>18,19</sup> For the scattering cross section, R-matrix theory does not guarantee it is a rational fraction in  $\sqrt{E}$ . However, a local Mittag-Leffler pole expansion of the scattering matrix can be performed that then yields local rational approximations for the cross section between thresholds.<sup>18,19</sup> This is at the core of the multipole representation of R-matrix cross sections.<sup>16,17</sup> We can thus assume to have such a form of the scattering cross section, which is flat at low energies and can have resonant structure:

$$\Sigma_s(E) = \Sigma_{s,0} + \frac{1}{\sqrt{E}} \Re \left[ \sum_{j=1}^J \frac{r_j^{c,s}}{\sqrt{E} - p_{s,j}} \right]. \quad (39)$$

This entails that the total cross section under this assumption takes, for real positive energies  $E \in \mathbb{R}_+$ , the following general form, which can describe very complex nuclear resonances:

$$\Sigma_t(E) = \Sigma_{s,0} + \frac{1}{\sqrt{E}} \Re \left[ \sum_{j=1}^J \frac{r_j^{c,t}}{\sqrt{E} - p_j} \right]. \quad (40)$$

Let us change variables:  $x \triangleq \sqrt{E}$ . From the cross-section pole representations in Eqs. (38), (39), and (40), the partial fraction decomposition of the  $D_S(x)$  ratio in  $x \triangleq \sqrt{E}$  space can be performed. A change of variables in the cross section does not alter their definition—that is,  $\sigma(x) = \sigma(E)$ —because they are mathematical functions. In contrast, the flux amplitudes  $\psi(E)$  are distributions, so a change of variables requires inclusion of the differential of the transformation, as the change of variables is defined in accordance with a measure:  $\psi(x)dx = \psi(E)dE$ . The same is true of the  $D_S(E)$  ratio, which acts as a downscattering distribution and for which the definition changes under a change of variable to include the differential of the transformation. Thus, under transformation  $x \triangleq \sqrt{E}$ , we have  $D_S(x)dx = D_S(E)dE$  so that  $D_S(x) = \frac{2\Sigma_s(x)}{x\Sigma_t^a(x)}$  from a change of variables:

$$\begin{aligned} \mathcal{I}_E^{E'} &\triangleq \int_E^{E'} D_S^a(E'') dE'' = \int_E^{E'} \frac{\Sigma_s(E'')}{E'' \Sigma_t^a(E'')} dE'' \\ &= \int_{\sqrt{E}}^{\sqrt{E'}} \frac{2\Sigma_s(x)}{x\Sigma_t^a(x)} dx = \int_{\sqrt{E}}^{\sqrt{E'}} D_S^a(x) dx. \end{aligned} \quad (41)$$

Since the total cross-section pole representation is Eq. (40), it follows that  $\sqrt{E}\Sigma_t^a(E)$  will be written as

$$\begin{aligned} \Re \left[ \sum_{j=1}^J \frac{r_j^{c,t}}{x - p_j} \right] &= \frac{\Re \left[ \sum_{j=1}^J r_j^{c,t} (x - p_j^*) \prod_{k \neq j} (x - p_k)(x - p_k^*) \right]}{\prod_{j=1}^J (x - p_j)(x - p_j^*)} \\ &= \frac{Q(x)}{P(x)}, \end{aligned}$$

where  $P(x)$  is a polynomial of degree  $2J$ . By multiplying the rational fraction in the integrand of Eq. (41) by the denominator  $P(x)$ , one finds that the  $D_S(x)$  irreducible form is

$$\begin{aligned} D_S(x) &\triangleq \frac{2\Sigma_s(x)}{x\Sigma_t^a(x)} \\ &= \frac{xP(x)\Sigma_s(x)}{P(x)[\alpha\sqrt{\frac{m_n}{2}} + x\Sigma_s] + \Sigma_R Q(x)}, \end{aligned} \quad (42)$$

which has  $N_p = \deg(P(x)) + 1$  poles and  $N_r = N_p - 1$  roots, with the number of poles being

$$N_p \triangleq 2J + 1, \quad (43)$$

and where  $m_n$  is the mass of the neutron. Upon partial fraction decomposition, the  $D_S^a$  ratio is thus expanded as the following sum of poles  $\{b_n\}$  and residues  $\{a_n\}$  in  $x = \sqrt{E}$  space:

$$D_S^a(x) = \sum_{n=1}^{N_p} \frac{a_n}{x - b_n}. \quad (44)$$

To compute the differential downscattering ratio integrals in Eq. (37),  $\mathcal{J}_{aE}^{E'}$  and  $\mathcal{J}_{\Sigma E}^{E'}$ , we take a similar approach and perform the partial fraction decomposition of  $\frac{\partial D_S^a}{\partial \alpha}(x)$  and  $\frac{\partial D_S^a}{\partial \Sigma}(x)$ . This is done by taking the partial differentials of the pole expansion in Eq. (44) and noting that they yield the following (where  $\Gamma$  stands for  $\alpha$ ,  $\Sigma$ , or any parameter):

$$\frac{\partial D_S^a}{\partial \Gamma}(x) = \sum_{n=1}^{N_p} \left[ \frac{\frac{\partial a_n}{\partial \Gamma}}{x - b_n} + \frac{a_n \frac{\partial b_n}{\partial \Gamma}}{(x - b_n)^2} \right]. \quad (45)$$

We now have poles of order two in  $x = \sqrt{E}$  space, the root finding (and residue estimation) of which will be discussed in Sec. V.

#### IV.B. Closed-Form Solutions for the $\alpha$ and $k$ Eigenproblems

Partial fraction decomposition in Eqs. (44) and (45) enable us to derive closed-form formulas for the reaction rate in Eq. (29) by noting that Eq. (36) readily integrates term-by-term to the following:

$$\mathcal{I}_E^{E'} = \sum_{n=1}^{N_p} a_n \ln \left( \frac{\sqrt{E'} - b_n}{\sqrt{E} - b_n} \right) \quad (46)$$

and that Eq. (37) integrates to

$$\mathcal{J}_{\Gamma_E^{E'}} = \sum_{n=1}^{N_p} \frac{\partial a_n}{\partial \Gamma} \ln \left( \frac{\sqrt{E'} - b_n}{\sqrt{E} - b_n} \right) + a_n \frac{\partial b_n}{\partial \Gamma} \left[ \frac{1}{\sqrt{E} - b_n} - \frac{1}{\sqrt{E'} - b_n} \right]. \quad (47)$$

Note that  $a_n$  and  $b_n$  are either real or that they come in complex conjugate pairs, and the imaginary parts cancel out so that Eq. (46) can also be expressed with real values:

$$\sum_{n=1}^{N_p} a_n \ln \left( \frac{\sqrt{E'} - b_n}{\sqrt{E} - b_n} \right) = \sum_{n=1}^{N_p} \left[ \Re[a_n] \ln \left| \frac{\sqrt{E} - b_n}{\sqrt{E_0} - b_n} \right| - \Im[a_n] \arg \left( \frac{\sqrt{E} - b_n}{\sqrt{E_0} - b_n} \right) \right].$$

The final results are derived from integrals in Eqs. (46) and (47), which entail the following closed-form solutions:

1. *The  $\alpha$  reaction rate from Eq. (29):*

$$R_\alpha(E) = \chi_0 F_\alpha \prod_{n=1}^{N_p} \left( \frac{\sqrt{E_\infty} - b_n}{\sqrt{E} - b_n} \right)^{a_n}. \quad (48)$$

Though the result of Eq. (48) is valid only for 0 K, R-matrix reaction cross sections, to our knowledge, it constitutes the first-ever explicit resolution of nuclear resonance self-shielding. Strikingly, no assumptions were made on the overlap of nuclear resonances, which is a traditionally unsolved challenge in nuclear reactor physics.<sup>5-9</sup> The same is true for the following closed-form result in Eq. (49).

1. *The near-criticality discrepancy of Eq. (32) between the  $\alpha$  and the  $k$  reaction rates:*

$$\frac{R_{\alpha,\Sigma} - R_{k,\Sigma}}{R_{k,\Sigma}}(E) \underset{|a| \ll 1}{\approx} \alpha \left[ \sum_{n=1}^{N_p} \frac{\partial a_n}{\partial \alpha} \ln \left( \frac{\sqrt{E_\infty} - b_n}{\sqrt{E} - b_n} \right) + a_n \frac{\partial b_n}{\partial \alpha} \left[ \frac{1}{\sqrt{E} - b_n} - \frac{1}{\sqrt{E_\infty} - b_n} \right] \right]. \quad (49)$$

## V. PERFORMING PARTIAL FRACTION DECOMPOSITION: NUMERICAL METHODS TO FIND THE POLES AND RESIDUES OF NUCLEAR CROSS SECTIONS

As stated above, in the neutral particle case without thresholds, nuclear cross sections can be expressed as rational fractions in  $v \propto \pm\sqrt{E}$  space, as in Eq. (40). This advanced nuclear physics result is established in the literature.<sup>18-20</sup> Furthermore, performing partial fraction decomposition as in Eqs. (44) and (45) was the key for us to construct the analytic solutions for the flux amplitude in Eq. (48) and the relative discrepancy in Eq. (49). However, performing such partial fraction decomposition is no trivial task. Algebraically, if the irreducible form of a rational fraction  $F(X)$  of the type in Eq. (45) is known,

$$F(X) = \frac{Q(X)}{P(X)} = \frac{Q(X)}{\prod_{n=1}^{N_p} (X - b_n)}, \quad (50)$$

to perform its partial fraction decomposition with poles of degree 2, as in Eq. (45),

$$F(X) = \sum_{n=1}^{N_p} \frac{a_{1,n}}{X - b_n} + \frac{a_{2,n}}{(X - b_n)^2}, \quad (51)$$

then one can first search for the poles  $\{b_n\}$  by means of a root-finding algorithm, after which the residues can be obtained, as follows:

$$a_{2,n} = \frac{Q(b_n)}{\prod_{k \neq n} (b_n - b_k)}$$

and

$$a_{1,n} = \frac{Q'(b_n)}{\prod_{k \neq n} (b_n - b_k)^2} - 2a_{2,n} \sum_{k \neq n} \frac{1}{b_n - b_k}. \quad (52)$$

In this case, we must first know the degree of the numerator and the denominator of the irreducible form in Eq. (42), which yields the correct number in Eq. (43) of poles  $N_p = 2(2N_\lambda + \sum_c \ell_c) + 1$  and roots  $N_r = N_p - 1$ . This result is established in works by Ducru et al.<sup>18,19</sup> and is significant since there are some pole cancellations occurring within the R-matrix theory that yield the cross-section expressions.

Once we know how many poles  $\{b_n\}$  to look for, Galois theory states that if  $N_p \geq 5$ , then they are a priori not solvable by radicals (see the Abel-Ruffini theorem). Therefore, a numerical algorithm is needed to find all the  $N_p$  poles in the complex plane. One such algorithm tested

in this work was the vector-fitting algorithm as explored by Peng et al.<sup>21</sup> However, for greater accuracy and certainty of convergence, numerical root finding of the denominator polynomial was performed in this work in the spirit of Ducru et al.<sup>22</sup> The MATLAB symbolic toolbox was leveraged to analytically calculate the polynomials for the numerator and the denominator of the  $D_s^a(v)$  factor. All of the cross-section definitions and the resulting polynomials are functions of  $v = \sqrt{E}$ . The exact rational fraction equations used for the cross sections will be presented in Sec. VI. After obtaining the analytic expressions for the polynomial in  $v$  of the denominator of the  $D_s^a(v)$  factor, an exact function for the Durand-Kerner method<sup>23,24</sup> was used. The Durand-Kerner method is an iterative method for the simultaneous determination of all the zeros of a polynomial  $P(x) = \prod_k^N (x - p_k)$ . The following fixed-point iteration is used to sequentially improve the estimate  $x_{k,j}$  of the root  $p_k$  until convergence:

$$x_{k,j+1} = x_{k,j} - \frac{P(x_j)}{\prod_{l < k} (x_{k,j} - x_{l,j+1}) \prod_{l > k} (x_{k,j} - x_{l,j})} . \quad (53)$$

While there is vast literature on numerical polynomial root finding,<sup>25–30</sup> most of it focuses on the computational complexity of such algorithms. Although it is not the most computationally efficient, we have found the Durand-Kerner method to be exceptionally effective at accurately finding all the roots of polynomials representing the poles of the  $D_s^a(v)$  factor for this benchmark. In trying different values for the resonance parameters and different numbers of resonances, we have never seen the Durand-Kerner method fail. The only practical caveat of the Durand-Kerner method is the numerical instability of Eq. (53) for high-order polynomials as demonstrated by Wilkinson.<sup>31</sup> For this reason, we solve the entire benchmark problem using MATLAB's variable precision arithmetic out to 250 digits.<sup>c</sup>

To obtain the closed-form solutions of Eqs. (48) and (49), partial fraction decomposition in Eqs. (44) and (45) must be performed, respectively. Both share the same poles, which were calculated using the Durand-Kerner method. To compute the residues  $\{a_n\}$  associated with the poles  $\{b_n\}$  of the downscattering ratio  $D_s^a(v)$  in Eq.

(44), we evaluate the numerator polynomial of irreducible form in Eq. (50) at the pole value  $b_n$  and divide it by the product of the difference of the given pole with all of the other poles,  $\prod_{k \neq n} (b_n - b_k)$ , as well as the analytically obtained leading coefficient of the denominator polynomial. For reasons similar to those applicable to the Wilkinson phenomenon,<sup>31</sup> this method is numerically unstable and thus also required the 250 digits of the variable precision arithmetic of MATLAB. The residues of the partial derivative  $\frac{\partial D_s^a}{\partial t}(v)$  in Eq. (45) are similarly obtained using the method in Eq. (52), in which we analytically calculated the derivative polynomial in the denominator by differentiating Eq. (42). As an alternative to the algebraic approach presented, Cauchy's residue theorem guarantees that it is also possible to take a complex analysis approach and perform the following contour integrals to obtain the residues of Eq. (51):

$$a_{1,n} = \frac{1}{2\pi i} \oint_{C_{b_n}} F(z) dz = \frac{\epsilon}{2\pi} \int_{\theta=0}^{2\pi} F(b_n + \epsilon e^{i\theta}) e^{i\theta} d\theta$$

and

$$a_{2,n} = \frac{1}{2\pi i} \oint_{C_{b_n}} (z - b_n) F(z) dz = \frac{\epsilon}{2\pi} \int_{\theta=0}^{2\pi} (b_n + \epsilon e^{i\theta}) F(b_n + \epsilon e^{i\theta}) e^{i\theta} d\theta .$$

The drawback with this approach is the high number of points along the contour that are required to achieve a given numerical accuracy,<sup>26,27,29,30</sup> which is why the algebraic approach was preferred for the purposes of this benchmark.

Only one more numerical computation is necessary to calculate this analytic benchmark: the numerical integration of the total number of fission neutrons. In this benchmark, whereas the flux  $\psi_k(E)$  in Eq. (48) is analytic (closed form), the calculation of the  $k$  eigenvalue does require numerical integration. We begin by rewriting Eq. (9) in the form

$$k = \frac{\chi(E) \int_{E_0}^{E_\infty} dE' v \Sigma_f(E') \psi_k(E')}{\Sigma_t(E) \psi_k(E) - \int_E^{E_\infty} dE' \frac{\Sigma_s(E')}{E'} \psi_k(E')} . \quad (54)$$

Equation (54) is valid for every point in energy  $E$ . To simplify the calculation,  $E = E_\infty$  was chosen, and in practice, Eq. (55) is used to compute the eigenvalue:

<sup>c</sup>In developing this analytic benchmark, the gracefulness of the numerical solution techniques was not the main objective. The elegance of the solution presented here is the compact parameterization of the flux (and reaction rate) in continuous energy in Eq. (48).



$$k = \frac{\chi(E_\infty) \int_{E_0}^{E_\infty} dE' v \Sigma_f(E') \psi_k(E')}{\Sigma_t(E_\infty) \psi_k(E_\infty)} . \quad (55)$$

Integral Eq. (55) is performed by first converting it to  $\log E$  space and then using Simpson's method with  $10^6$  points in  $\log E$ , equally spaced between  $E_0$  and  $E_\infty$ . The  $\alpha$  eigenvalue is defined through the implicit relationship in Eq. (30). To find the  $\alpha$  eigenvalue, we solve the  $k$ -eigenvalue problem with an  $\alpha$ -dependent total cross section  $\Sigma_t^\alpha$ . We use the secant method with some bounding initial values for  $\alpha$  and iterate until we find an  $\alpha$  eigenvalue, for which  $k = 1$ .

## VI. NUMERICAL BENCHMARK, DEFINITION AND RESULTS

This section provides computed reference values for this analytic neutron transport benchmark.

### VI.A. Quantitative Description of the Benchmark

In a compromise between a realistic problem and simplicity, we have chosen to define our benchmark problem as shown below.

The input parameters in Table I are combined with the set of equations (56), (57), and (58) to form the definition of our benchmark:

$$v = \sqrt{E} ,$$

$$k = \rho_0 v ,$$

$$\Gamma_n(v) = \Gamma_n \frac{v}{\sqrt{E_\lambda}} , \quad (56)$$

$$\begin{aligned} \Gamma_t(v) &= \Gamma_n(v) + \Gamma_\gamma + \Gamma_f , \\ d &= (v^2 - E_\lambda)^2 + (\Gamma_t(v)/2)^2 , \end{aligned} \quad (57)$$

$$\rho = ka_c ,$$

$$\begin{aligned} \sigma_s &= 4\pi a_c^2 + \frac{g_f \pi}{d} \\ &\left[ \frac{\Gamma_n(v)^2}{k^2} + \frac{4a_c(v^2 - E_\lambda)\Gamma_n(v)}{k} - 2a_c^2 \Gamma_n(v) \Gamma_t(v) \right] , \end{aligned} \quad (58)$$

$$\sigma_g = \frac{g_f \pi \Gamma_n(v) \Gamma_\gamma}{k^2 d} ,$$

and

$$\sigma_f = \frac{g_f \pi \Gamma_n(v) \Gamma_f}{k^2 d} .$$

Except for Eq. (58), all of Equations presented immediately above are exact cross-section equations from R-matrix theory for the resonance parameters given in Table I. The Single-Level Breit-Wigner resonance formalism yields identical equations for the single resonance case. Equations (56) and (57) call out the explicit energy dependence of the resonance width compared to the values fixed at the resonance energy in Table I. Furthermore, in Eq. (58), we have taken the Taylor expansion of the phase-shift factor assuming that  $\rho \ll 1$ . To enforce this for the analytic benchmark for  $[E \in [10^{-5}, 2 \times 10^7]]$ , the scattering radii for both  $^{239}\text{Pu}$  and  $^{238}\text{U}$  were reduced by three orders of magnitude.

Only the scattering, fission, and total cross sections of the homogeneous material are necessary to compute this analytic benchmark. Since the material is homogeneous, all rescalings of the number density  $N$  are equivalent. Therefore, the units of  $N$  are not given in Table I. Since the value of  $v$  is 0 for the capture isotope, the total fission cross section is given only by the fission isotope. The total scattering cross section is given by the sum of the resonance scattering from the fission and capture isotopes and the constant in energy scattering of the scattering isotope. The total cross section is the sum of the total fission and total scattering plus the sum of the resonance capture cross sections from the fission and capture isotopes. Figure 1 presents the plot of the cross sections for this problem. For numerical testing purposes, Table II reports the values of the cross sections at several energies.

### VI.B. Evaluation of the Benchmark Quantities

The calculated  $k$  eigenvalue is 1.00000, within numerical accuracy of less than 1 pcm. That is, using the variable precision arithmetic in MATLAB, the  $k$  eigenvalue calculates to unity with a round-off error in the sixth decimal point and beyond.

The  $D_s$  factor is plotted in Fig. 2, and the flux is plotted in Fig. 3. However, neither figure should be considered to include benchmark quantities but is provided merely for visual reference. Rather, the  $D_s$  factor should be computed from Eq. (44) using the values in Table III, and the flux



TABLE I  
Quantitative Description of the Benchmark Inputs

Material	Fission Isotope	Capture Isotope	Scattering Isotope
Description	Lowest lying resonance of $^{239}\text{Pu}$	Lowest lying s-wave resonance of $^{238}\text{U}$	Flat scattering cross section
$N$	1.00	0.124954	0.008340505
$\nu$	2.88	0	0
$g_J$	3/4	1	
$E_\lambda$ (eV)	2.956243e-1	6.674280e+0	
$\Gamma_n$ (eV)	7.947046e-5	1.492300e-3	
$\Gamma_\gamma$ (eV)	3.982423e-2	2.271100e-2	
$\Gamma_f$ (eV)	5.619673e-2	9.880000e-9	
$a_c$ ( $10^{-12}$ cm)	9.410000e-4	9.480000e-4	
$\sigma_s$ (b)			20.0
$\rho_0$	$0.002196807122623 \times 1/2$	$0.002196807122623 \times 1/2$	$0.002196807122623 \times 1/2$

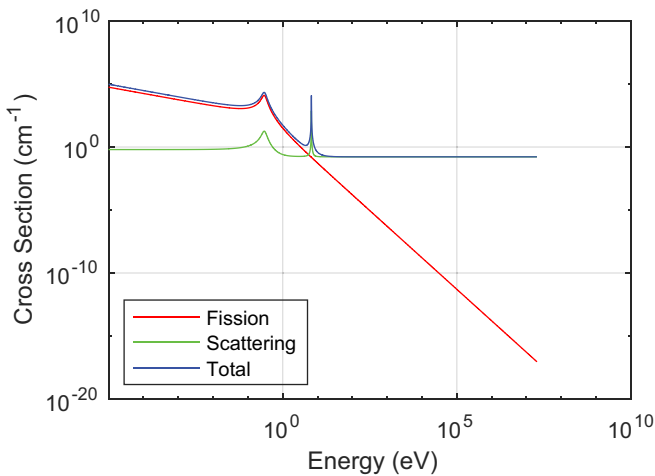


Fig. 1. Cross sections for the analytic benchmark problem.

should be computed using Eq. (48). Remember that the flux is the eigenfunction of the solution, so the absolute magnitude is arbitrary.

In order to make a comparison with a Monte Carlo radiation transport code, the reader would calculate the continuous-energy flux for this benchmark using Eq. (48) and then group the flux into the same energy structure as the bins used for the flux tally in the Monte Carlo code. In this way, we have provided a very general benchmark problem that can be adapted to any energy group structure. For ease of normalization we recommend comparing the ratio between the flux in different energy groups rather than the absolute values.

The reaction rates are provided in Fig. 4 for ease of comprehension. Table IV mirrors Table II and is an example of the values of the reaction rates on the

TABLE II  
Select Cross-Section Values for the Analytic Benchmark

Energy (eV)	Fission ( $\text{cm}^{-1}$ )	Scattering ( $\text{cm}^{-1}$ )	Total ( $\text{cm}^{-1}$ )
0.00001	$5.6556 \times 10^4$	$6.3041 \times 10^{-1}$	$9.6665 \times 10^4$
0.01000	$1.9122 \times 10^3$	$6.6248 \times 10^{-1}$	$3.2690 \times 10^3$
0.29562	$1.2778 \times 10^4$	$1.8240 \times 10^1$	$2.1852 \times 10^4$
6.67425	$1.5751 \times 10^{-1}$	$7.4146 \times 10^2$	$1.2024 \times 10^4$
100.000	$1.6136 \times 10^{-4}$	$1.6686 \times 10^{-1}$	$1.6718 \times 10^{-1}$
$2.0 \times 10^7$	$8.9673 \times 10^{-18}$	$1.6682 \times 10^{-1}$	$1.6682 \times 10^{-1}$

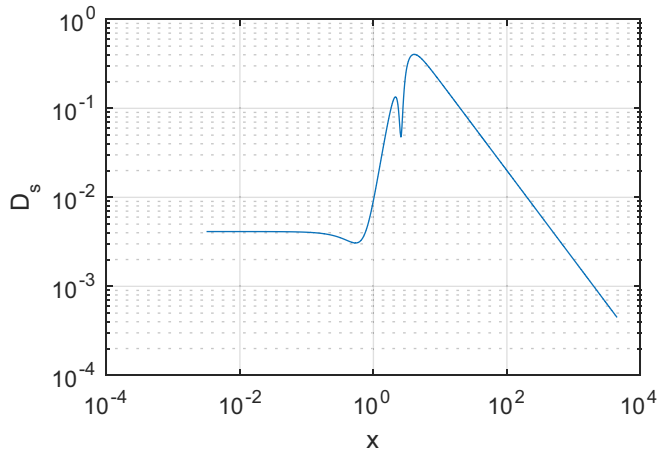
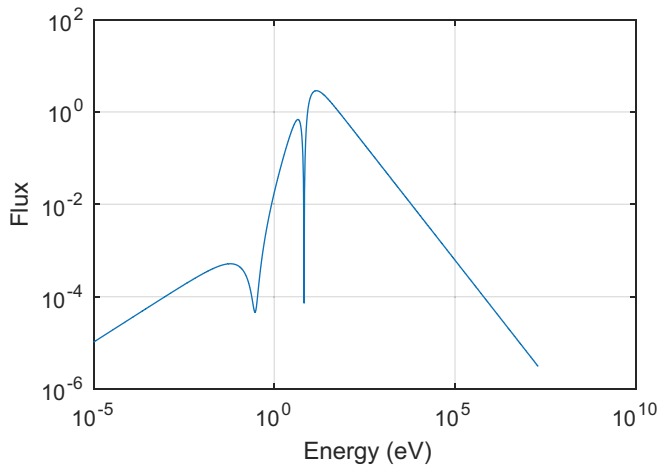
Fig. 2. The  $D_s$  factor for the analytic benchmark problem.

Fig. 3. Flux for the analytic benchmark problem. The benchmark flux values should be computed using Eq. (48) and the values in Table III.

same energy grid. Table IV is generated by plugging the parameters from Table III into Eq. (48). Once again, this analytic benchmark defines parameterization of the continuous-energy reaction rate and flux.

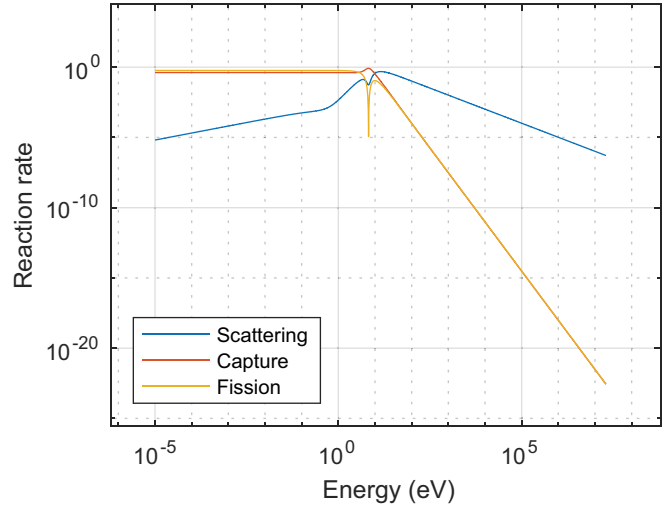


Fig. 4. Reaction rates for the analytic benchmark.

## VI.C. Verification Results

Using the ENDF-formatted input files provided in the online supplement, the  $k$  eigenvalue has been verified to within 10 pcm using the KENO module of SCALE 6.2.3 (Ref. 12), as well as OpenMC (Ref. 13) with 7000 generations and 10 000 particles per generation. The flux profile was also verified using a custom-made 0-D analog Monte Carlo transport code using  $10^9$  particle histories.

## VII. NUMERICAL EXPERIMENTS AROUND THE BENCHMARK

This section introduces the comparison between the deviations in the flux spectra in response to a differential change in the density of the capture isotope. Figure 5 presents the graphical connections between the three points and the differences between the fluxes at those points. Point 1 is the critical configuration of the analytic benchmark, which is defined in this work with  $k = 1$  and  $\alpha = 0$ . In Point 1, the  $k$  flux  $\psi_k(E)$  and the  $\alpha$  flux  $\psi_\alpha(E)$  are identical. The flux is shown in Fig. 3. Point 2, which is depicted higher on the

TABLE III

Poles  $\{b_n\}$  and Residues  $\{a_n\}$  for the  $D_s$  Factor (44) and the Flux (48)

Poles $\{b_n\}$ ( $\sqrt{\text{eV}}$ )	Residues $\{a_n\}$ (Dimensionless)
$-3.231937213213652$ $-2.359656288731372 \pm 0.413452243806859i$ $-0.895084182048309 \pm 2.614122283641052i$ $2.541844625130926 \pm 0.407340321738616i$ $2.328864452255582 \pm 1.542044207418896i$	$0.240755381502399$ $0.067887896840442 \mp 0.029089816104523i$ $0.418394273669056 \mp 0.007622138370498i$ $-0.036967969300154 \pm 0.052079653916755i$ $0.430308108039457 \mp 0.003140381126088i$

TABLE IV  
 Select Reaction Rate Values for the Analytic Benchmark\*

Energy (eV)	Fission	Scattering	Capture
0.00001	$5.8506 \times 10^{-1}$	$6.5215 \times 10^{-6}$	$4.1492 \times 10^{-1}$
0.01000	$5.8472 \times 10^{-1}$	$2.0258 \times 10^{-4}$	$4.1466 \times 10^{-1}$
0.29562	$5.8361 \times 10^{-1}$	$8.3304 \times 10^{-4}$	$4.1359 \times 10^{-1}$
6.67425	$1.1614 \times 10^{-5}$	$5.4674 \times 10^{-2}$	$8.3189 \times 10^{-1}$
100.000	$9.9244 \times 10^{-5}$	$1.0262 \times 10^{-1}$	$1.0047 \times 10^{-4}$
$2.0 \times 10^7$	$2.7657 \times 10^{-23}$	$5.1452 \times 10^{-7}$	$2.6959 \times 10^{-23}$

\*The absolute magnitude is arbitrary. Only the ratios between different reactions and different points in energy are relevant.

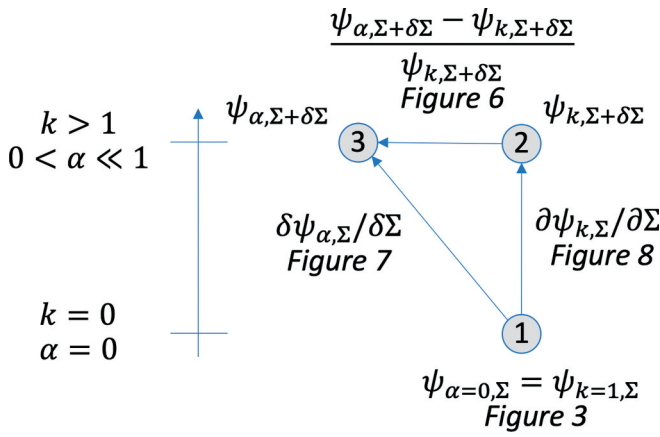


Fig. 5. Flux changes due to a change in the density of the capture isotope.

vertical ( $k$ -) axis, represents the flux calculated using a  $k$ -eigenvalue solve for a differential decrease in the density of the capture isotope. The difference between the  $k$  fluxes in Point 1 and Point 2 is calculated using Eq. (34) and is depicted in Fig. 8 (discussed later). Point 3 is in the same physical configuration as Point 2, but it refers to the solution of the  $\alpha$  eigenproblem. The difference between the fluxes in Point 2 and Point 3 is computed using Eq. (32) and is shown in Fig. 6. Finally, the difference in the fluxes between Point 3 and Point 1 is calculated using Eq. (33) and is shown in Fig. 7. Note that since Fig. 7 depicts the interdependence between Eqs. (32), (33), and (34) around the criticality Point 1 ( $\alpha = 0$ ,  $k = 1$ ), the perturbed value of  $\alpha$  is equal to the small perturbation  $\delta\alpha$  close to criticality; that is,  $\alpha(\Sigma + \delta\Sigma) = \alpha(\Sigma) + \delta\alpha + \mathcal{O}(|\delta\Sigma|^2)$  where  $\frac{\delta\alpha}{\delta\Sigma}$  is the differential in Eq. (33).

All of the results in Secs. VII.A and VII.B have been verified by direct perturbation of the flux solutions.

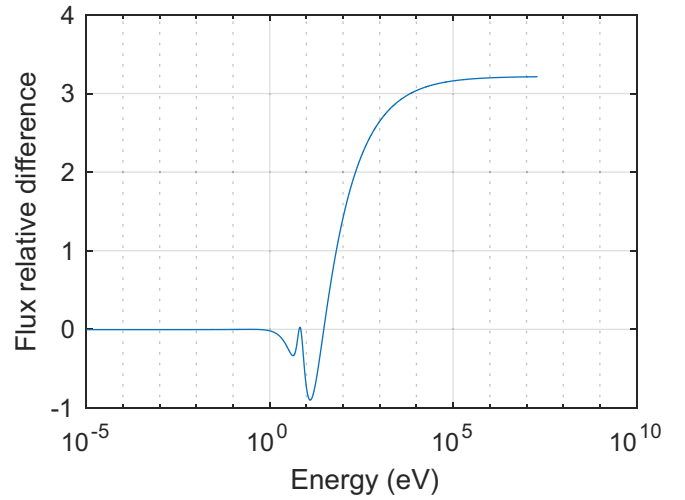


Fig. 6. First-order relative flux difference in  $\psi_k$  for a perturbation of the number density  $N$  of the capture isotope from the critical state. The vertical axis shows  $\lim_{\delta N \rightarrow 0} \frac{1}{\psi_{k(N)}(E)} \frac{\psi_{k(N+\delta N)}(E) - \psi_{k(N)}(E)}{\delta N}$ .

### VII.A. Discrepancy Between the $\psi_\alpha(E)$ and $\psi_k(E)$ Flux Amplitudes Away From Criticality

Based on the derivations presented in Secs. II.D and II.E, Fig. 6 shows the first-order discrepancy between  $\psi_\alpha(E)$  and  $\psi_k(E)$  per unit alpha for slight perturbations off the critical state of the benchmark defined above,  $|\alpha| \ll 1$ .

Figure 6 shows the discrepancy in the flux that will be created using a criticality code to calculate a noncritical system. This even applies to a system that is only slightly noncritical.

### VII.B. $\psi(E)$ Flux Oscillations Around Criticality due to Changes in Absorption

Unlike Fig. 6, Fig. 7 shows how the alpha flux will change for a critical system if the number density of the capture isotope is changed.

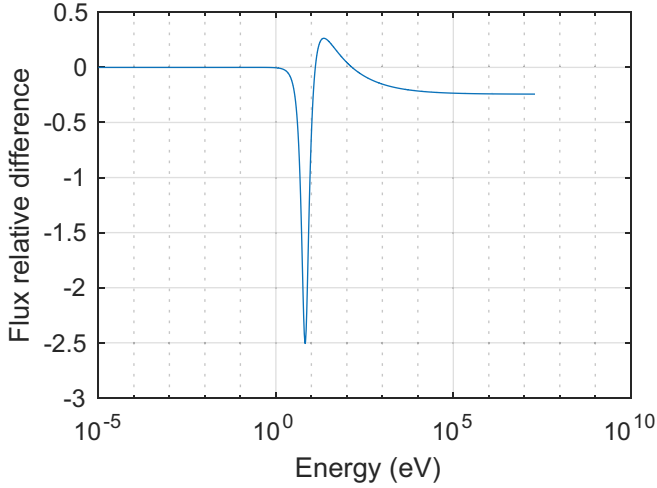


Fig. 7. First-order relative difference between the  $\psi_\alpha(E)$  and the  $\psi_k(E)$  per unit alpha for slight perturbations ( $|\alpha| \ll 1$ ) off the critical state of the analytic benchmark. The vertical axis shows  $\lim_{\delta\alpha \rightarrow 0} \frac{1}{\psi_k(E)} \frac{\psi_{\alpha+\delta\alpha}(E) - \psi_k(E)}{\delta\alpha}$ .

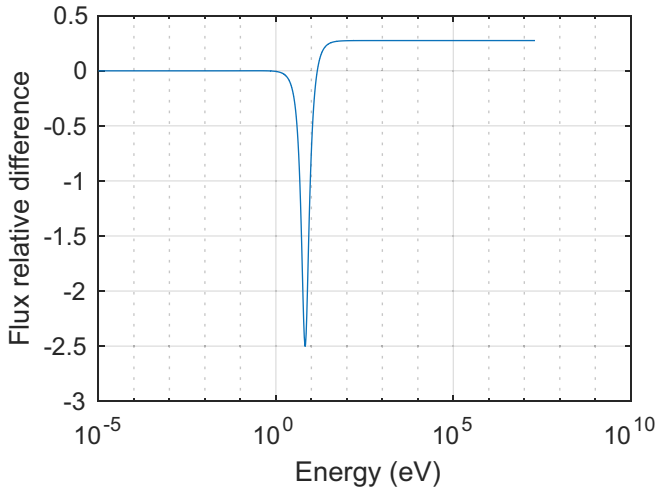


Fig. 8. First-order relative flux difference in  $\psi_\alpha$  for a perturbation of the number density  $N$  of the capture isotope from the critical state. The vertical axis shows:  $\lim_{\delta N \rightarrow 0} \frac{1}{\psi_{\alpha(N)}(E)} \frac{\psi_{\alpha(N+\delta N)}(E) - \psi_{\alpha(N)}(E)}{\delta N}$ .

Perhaps the most striking observation from this work is the contrast between the change of  $\psi_\alpha$  and  $\psi_k$  for a change of the number density of the capture isotope for the critical configuration. The relative difference in  $\psi_k$  is presented in Fig. 7.

The difference between Figs. 7 and 8 is the discrepancy between using  $k$ -eigenvalue and  $\alpha$ -eigenvalue codes to compute derivatives with respect to changes in the nuclear data. A  $k$ -eigenvalue code will predict that for a change in the number density of the capture isotope, the flux will change as shown

in Fig. 8 whereas using the  $\alpha$ -eigenvalue code,  $\psi_\alpha$  will change as shown in Fig. 7. Even though they both start from the same flux at  $k = 1, \alpha = 0$ , the initial response of the energy-dependent flux to a change in the density of the capture isotope is different depending on which model one chooses.

## VIII. CONCLUSION

In this work, we have derived the equations for the analytic solution of the flux for a 0-D (infinite homogeneous) neutron Boltzmann transport downscattering problem as shown in Eq. (13) with a step fission spectrum as shown in Eq. (28) and an arbitrary number of nuclear resonances for cross sections with neutral particles, no threshold, and 0 K reaction. Equation (16) provides the solution for both the time-dependent  $\alpha$  flux and the critical  $k$  flux. To our surprise, we found that in this problem, the  $k$  flux is independent of the eigenvalue and that the  $k$  eigenvalue is computed by an integral of the flux while the  $\alpha$  flux and the  $\alpha$  eigenvalue are tied together in an implicit relationship. To the best of our knowledge, this is the first explicit resolution of the nuclear resonance self-shielding phenomenon, albeit at 0 K.

Based on our derivations, we have defined a benchmark problem for other computation methods. The benchmark is defined in Sec. VI while the methods used to compute the results are detailed in Secs. IV and V. For most modern computational methods in reactor physics, the benchmark is really defined only as an infinite homogeneous medium with three materials given by the ENDFs in the online supplement and the number densities given in Table I. The benchmark quantities are the  $k$  eigenvalue of unity to less than 1 pcm, and the flux is calculated using Eq. (48), with the pole and residue values documented in Table III.

We hope this work provides new insights into the differences between the time-dependent  $\alpha$  flux and the critical  $k$  flux. In Sec. VII, we show the relative difference in the flux calculated by a  $k$ -eigenvalue code for near-critical systems compared to the flux calculated by an  $\alpha$ -eigenvalue code.

## SUPPLEMENTAL MATERIAL

Supplemental data for this article can be accessed online at [publisher's website](#).

## ACKNOWLEDGMENTS

The authors are truly indebted to Andrew Holcomb of Oak Ridge National Laboratory for his assistance in validating the analytic benchmark problem with SCALE 6.2.3.

The second author, P. Ducru, was supported by the Consortium for Advanced Simulation of Light Water Reactors, an Energy Innovation Hub for Modeling and Simulation of Nuclear Reactors under U.S. Department of Energy contract number DE-AC05-00OR22725.

## References

1. P. REUSS, *Neutron Physics*, EDP Sciences, ISBN 2-7598-0041-4.
2. A. HÉBERT, *Applied Reactor Physics*, Presses Internationales Polytechnique, ISBN 978-2-553-01436-9.
3. G. ALLAIRE et al., “Transport et Diffusion,” École Polytechnique.
4. G. I. BELL and S. GLASSTONE, *Nuclear Reactor Theory*, U.S. Atomic Energy Commission, Van Nostrand Reinhold Company, Library of Congress Catalog Card Number 73-122674.
5. N. A. GIBSON, “Novel Resonance Self-Shielding Methods for Nuclear Reactor Analysis,” PhD Thesis, Massachusetts Institute of Technology, Department of Nuclear Science and Engineering (2016); <http://hdl.handle.net/1721.1/103658> (current as of Oct. 1, 2020).
6. P. REUSS, “A Generalization of the Livolant-Jeanpierre Theory for Resonance Absorption Calculation,” *Nucl. Sci. Eng.*, **92**, 2, 261 (1986); <https://doi.org/10.13182/NSE86-A18174>.
7. M. L. WILLIAMS, “Resonance Self-Shielding Methodologies in SCALE 6,” *Nucl. Technol.*, **174**, 2, 149 (2011); <https://doi.org/10.13182/NT09-104>.
8. G. CHIBA, A. TSUJI, and T. NARABAYASHI, “Resonance Self-Shielding Effect in Uncertainty Quantification of Fission Reactor Neutronics Parameters,” *Nucl. Eng. Technol.*, **46**, 3, 281 (2014); <https://doi.org/10.5516/NET.01.2014.707>.
9. J. LI et al., “Resonance Self-Shielding Treatment and Analysis of Resonance Integral Tables for Fully Ceramic Micro-Encapsulated Fuels with the Embedded Self-Shielding Method,” *Ann. Nucl. Energy*, **112**, 450 (2018); <https://doi.org/10.1016/j.anucene.2017.10.027>.
10. J.-P. M. PERAUD, C. D. LANDON, and N. G. HADJICONSTANTINO, “Monte Carlo Methods for Solving the Boltzmann Transport Equation,” *Ann. Rev. Heat Transfer*, **17**, 205 (2014); <https://doi.org/10.1615/AnnualRevHeatTransfer.2014007381>.
11. “MCNP Users Manual: Code Version 6.2,” C. J. WERNER, Ed., Los Alamos National Laboratory (2017); [https://mcnp.lanl.gov/pdf\\_files/la-ur-17-29981.pdf](https://mcnp.lanl.gov/pdf_files/la-ur-17-29981.pdf) (current as of Oct. 1, 2020).
12. S. GOLUOGLU et al., “Monte Carlo Criticality Methods and Analysis Capabilities in SCALE,” *Nucl. Technol.*, **174**, 2, 214 (2011); <https://doi.org/10.13182/NT10-124>.
13. P. K. ROMANO et al., “OpenMC: A State-of-the-Art Monte Carlo Code for Research and Development,” *Ann. Nucl. Energy*, **82**, 90 (2015); <https://doi.org/10.1016/j.anucene.2014.07.048>.
14. C. BLOCH, “Une formulation unifiée de la théorie des réactions nucléaires,” *Nucl. Phys.*, **4**, 503 (1957); [https://doi.org/10.1016/0029-5582\(87\)90058-7](https://doi.org/10.1016/0029-5582(87)90058-7).
15. A. M. LANE and R. G. THOMAS, “R-Matrix Theory of Nuclear Reactions,” *Rev. Mod. Phys.*, **30**, 2, 257 (1958); <https://doi.org/10.1103/RevModPhys.30.257>.
16. B. FORGET, S. XU, and K. SMITH, “Direct Doppler Broadening in Monte Carlo Simulations Using the Multipole Representation,” *Ann. Nucl. Energy*, **64**, 78 (2014); <https://doi.org/10.1016/j.anucene.2013.09.043>.
17. C. JOSEY et al., “Windowed Multipole for Cross Section Doppler Broadening,” *J. Comput. Phys.*, **307**, 715 (2016); <https://doi.org/10.1016/j.jcp.2015.08.013>.
18. P. DUCRU et al., “Scattering Matrix Pole Expansions & Invariance with Respect to R-Matrix Parameters” (2019); <https://arxiv.org/abs/1903.02661> (current as of Oct. 1, 2020).
19. P. DUCRU et al., “Windowed Multipole Representation of R-Matrix Cross Sections,” *Phys. Rev. C* (2019) (to be published).
20. R. N. HWANG, “A Rigorous Pole Representation of Multilevel Cross Sections and Its Practical Applications,” *Nucl. Sci. Eng.*, **96**, 3, 192 (1987); <https://doi.org/10.13182/NSE87-A16381>.
21. X. PENG et al., “Converting Point-Wise Nuclear Cross Sections to Pole Representation Using Regularized Vector Fitting,” *Comput. Phys. Commun.*, **224**, 52 (2018); <https://doi.org/10.1016/j.cpc.2017.12.004>.
22. P. DUCRU et al., “On Methods for Conversion of R-Matrix Resonance Parameters to Multi-Pole Formalism,” *Proc. PHYSOR 2016*, Sun Valley, Idaho, May 1–5, 2016, p. 2138, American Nuclear Society (2016).
23. E. DURAND, “Solutions numériques des équations algébriques,” Vol. 1, *Equations Du Type  $F(x) = 0$ : Racines D’un Polynome*, Masson et Cie, Paris.
24. M. PETKOVIC, *Iterative Methods for Simultaneous Inclusion of Polynomial Zeros*, Vol. 1387, Springer-Verlag Berlin Heidelberg (1989).
25. O. ABERTH, “Iteration Methods for Finding All Zeros of a Polynomial Simultaneously,” *Math. Comput.*, **27**, 122, 339 (1973); <https://www.ams.org/journals/mcom/1973-27-122/S0025-5718-1973-0329236-7/S0025-5718-1973-0329236-7.pdf> (current as of Oct. 1, 2020).
26. A. SCHÖNHAGE, “The Fundamental Theorem of Algebra in Terms of Computational Complexity” (1982); <http://cite-seerx.ist.psu.edu/viewdoc/download?doi=10.1.1.123.3313&rep=rep1&type=pdf> (current as of Oct. 1, 2020).
27. X. GOURDON, “Combinatoire, Algorithmique et Géométrie des Polynômes,” PhD Thesis, École Polytechnique (1996).

28. P. D. PROINOV and S. I. IVANOV, “On the Convergence of Halley’s Method for Multiple Polynomial Zeros,” *Mediterr. J. Math.*, **12**, 555 (2015); <https://doi.org/10.1007/s00009-014-0400-7>
29. V. Y. PAN, “Optimal and Nearly Optimal Algorithms for Approximating Polynomial Zeros,” *Comput. Math. Appl.*, **31**, 12, 97 (1996); [https://doi.org/10.1016/0898-1221\(96\)00080-6](https://doi.org/10.1016/0898-1221(96)00080-6).
30. V. Y. PAN, “Approximating Complex Polynomial Zeros: Modified Weyl’s Quadtree Construction and Improved Newton’s Iteration,” *J. Complexity*, **16**, 1, 213 (2000); <https://doi.org/10.1006/jcom.1999.0532>.
31. J. H. WILKINSON, “The Evaluation of the Zeros of Ill-Conditioned Polynomials,” *Numer. Math.*, **1**, 1, 150 (1959); <https://doi.org/10.1007/BF01386381>